Molecular & Biochemical Parasitology 184 (2012) 63–70

Contents lists available at SciVerse ScienceDirect

Molecular & Biochemical Parasitology

Characterization of the M32 metallocarboxypeptidase of *Trypanosoma brucei*: Differences and similarities with its orthologue in *Trypanosoma cruzi*

Alejandra P. Frasch[a], Adriana K. Carmona[b], Luiz Juliano[b], Juan J. Cazzulo[a], Gabriela T. Niemirowicz[a,*]

[a] *Instituto de Investigaciones Biotecnológicas "Dr. Rodolfo Ugalde"-Instituto Tecnológico Chascomús, UNSAM-CONICET, Campus Miguelete, Av. 25 de Mayo y Francia, 1650 San Martín, Buenos Aires, Argentina*
[b] *Departamento de Biofísica, Universidade Federal de São Paulo, Rua 3 de maio 100, 04044-020, São Paulo, SP, Brazil*

ARTICLE INFO

Article history:
Received 14 February 2012
Received in revised form 20 April 2012
Accepted 23 April 2012
Available online 28 April 2012

Keywords:
Trypanosoma brucei
Carboxypeptidase
M32 family
FRET peptides
Trypanosoma cruzi
Peptidase

ABSTRACT

Metallocarboxypeptidases (MCP) of the M32 family of peptidases have been identified in a number of prokaryotic organisms but they are absent from eukaryotic genomes with the remarkable exception of those of trypanosomatids. The genome of *Trypanosoma brucei*, the causative agent of Sleeping Sickness, encodes one such MCP which displays 72% identity to the characterized *Tc*MCP-1 from *Trypanosoma cruzi*. As its orthologue, *Tc*MCP-1, *Trypanosoma brucei* MCP is a cytosolic enzyme expressed in both major stages of the parasite. Purified recombinant *Tb*MCP-1 exhibits a significant hydrolytic activity against the carboxypeptidase B substrate FA (furylacryloil)-Ala-Lys at pH 7.0–7.8 resembling the *T. cruzi* enzyme. Several divalent cations had little effect on *Tb*MCP-1 activity but increasing amounts of Co^{2+} inhibited the enzyme. Despite having similar tertiary structure, both protozoan MCPs display different substrate specificity with respect to P1 position. Thus, *Tc*MCP-1 enzyme cleaved Abz-FVK-(Dnp)-OH substrate (where Abz: *o*-aminobenzoic acid and Dnp: 2,4-dinitrophenyl) whereas *Tb*MCP-1 had no activity on this substrate. Comparative homology models and sequence alignments using *Tc*MCP-1 as a template led us to map several residues that could explain this difference. To verify this hypothesis, site-directed mutagenesis was undertaken replacing the *Tb*MCP-1 residues by those present in *Tc*MCP-1. We found that the substitution A414 M led *Tb*MCP-1 to gain activity on Abz-FVK-(Dnp)-OH, thus showing that this residue is involved in specificity determination, probably being part of the S1 sub-site. Moreover, the activity of both protozoan MCPs was explored on two vasoactive compounds such as bradykinin and angiotensin I resulting in two different hydrolysis patterns.

1. Introduction

Carboxypeptidases are enzymes that cleave the C-terminal amino acid residue from peptides and proteins. This hydrolysis step may result in substrate activation or degradation [1]. Regardless the outcome, this activity belongs to two major catalytic classes of proteases, namely metallocarboxypeptidases (MCPs) and serine carboxypeptidases [1]. MCPs are ubiquitous in nature and typically have a single zinc ion bound to the active site. Among carboxypeptidases, the family M14 is the most extensively studied group. This family includes several enzymes which participate in diverse processes such as blood coagulation and fibrinolysis, inflammation, innate immunity response, food digestion and pro-hormone and neuropeptide processing [2].

Previous studies on *Thermus aquaticus*, an extremely thermophilic bacterium, led to the identification of a new zinc-dependent MCP [3]. Contrary to archetypical M14 peptidases, *Thermus aquaticus* carboxypeptidase (*Taq*CP) was distinct in both size and sequence. *Taq*CP contained a HEXXH signature which is a conserved sequence found in the active site of neutral metalloendopeptidases, but not described previously in a carboxypeptidase. These facts led to the placement of *Taq*CP in the newly formed M32 family of MCPs [4]. Later studies performed on other members of this family also confirmed that this group of enzymes had also strong topological similarity with archaeal, bacterial and mammalian endopeptidases including angiotensin I-converting enzyme (ACE), neurolysin and thimet oligopeptidase [4,5].

Abbreviations: BSA, bovine serum albumin; BSF, bloodstream form; CPB, carboxypeptidase B; E64, L-transepoxysuccinyl-leucylamido-[4-guanidino] butane; FRET, Fluorescence Energy Resonance Transfer; GEMSA, guanidinoethylmercaptosuccinic acid; IMAC-Ni^{2+}, immobilized metal affinity chromatography using Ni^{2+}; MOPS, 3-(N-morpholino) propanesulfonic acid; NP40, nonyl phenoxypolyethoxylethanol; Plummer's inhibitor, DL-2-mercaptomethyl-3-guanidinoethylthiopropanoic acid; PMSF, phenylmethylsulfonyl fluoride; PCF, procyclic form; TD Buffer, trypanosome dilution buffer.

* Corresponding author at: Instituto de Investigaciones Biotecnológicas "Dr. Rodolfo Ugalde"-Instituto Tecnológico de Chascomús (IIB-INTECH, UNSAM-CONICET), Campus Miguelete, Av. 25 de Mayo y Francia, 1650 San Martín, Buenos Aires, Argentina. Tel.: +54 11 4006 1500; fax: +54 11 4006 1559.
E-mail address: gniemiro@iibintech.com.ar (G.T. Niemirowicz).

0166-6851/$ – see front matter © 2012 Elsevier B.V. All rights reserved.
http://dx.doi.org/10.1016/j.molbiopara.2012.04.008

But not only the structural similarity to endopeptidases as well as their broad substrate specificity were the new features of these peptidases; their phylogenetic distribution was also quite peculiar. Sequence alignments have identified M32 family members in species from a very limited phylogenetic range. These include bacteria, archaea, some green algae and trypanosomatids, but not metazoa, suggesting that the genes have been acquired by horizontal gene transfer or retained for some special function that is no longer essential for higher organisms [6].

The Trypanosomatidae family includes several vector-borne protist parasites, causing human and veterinary diseases. The human parasites include a number of species in the genera *Leishmania* and *Trypanosoma*. In *Trypanosoma*, the two major human parasites are *T. cruzi*, the causative agent of Chagas' disease, and *T. brucei*, the causative agent of the Human African trypanosomiasis (HAT) or Sleeping Sickness. Both parasites are responsible for over 60,000 deaths per year in Latin America and Sub-Saharan Africa, respectively. For these infections no vaccines are available, and their treatment is dependent on a small number of drugs that have limited efficacy and can cause severe side effects [7]. These limitations make urgent the need to develop new drugs, more efficient, less toxic and more affordable [8]. In this context the study of peptidases has acquired considerable importance since several works have shown that many parasites deploy proteinases to accomplish both "housekeeping" tasks common to many eukaryotes as well as functions highly specific to the parasite life style. Host cell invasion and egress, encystation, excystation, catabolism of host proteins, differentiation, cell cycle progression, cytoadherence, and both stimulation and evasion of host immune responses are some processes in which this group of enzymes has been shown to be involved [9]. Thus, the possibility of developing selective inhibitors of key proteases of pathogenic parasites is currently explored as a novel chemotherapeutic strategy [9].

Herein we focus on *T. brucei*, an extracellular parasite, transmitted by the bite of the tsetse fly (*Glossina* spp.). The disease caused by this protozoan progresses from non-specific signs to typical symptoms such as wake–sleep cycle alteration and neurological dysfunction, leading to death in untreated patients [10]. In this work we report the cloning, purification and biochemical characterization of an MCP belonging to the M32 family (*Tb*MCP-1) from *T. brucei* Lister 427. These results add to our knowledge of the peptidases present in *T. brucei* and may offer a new target for the development of a rational chemotherapy against trypanosomiasis.

2. Materials and methods

2.1. Materials

Peptide substrates were purchased from Sigma–Aldrich and Bachem Bioscience, except for those with the structure Abz-XXK(Dnp)-OH [Abz: *o*-aminobenzoic acid; K(Dnp): N′,2,4-dinitrophenyllysine, and X different amino acid residues], which were synthesized as described in Ref. [11]. All other reagents were purchased from Sigma unless otherwise stated.

2.2. Trypanosome strains and culture conditions

The *T. brucei* bloodstream form (BSF) Lister 427 "single marker" trypanosome cell line (T7RNAPol TetR NEO) and the procyclic form (PCF) 29–13 cell line (T7RNAPol NEO TetR HYG) [12] were gifts from G.A.M. Cross (Rockefeller University). BSF cells were maintained in HMI-9 medium supplemented with 20% heat-inactivated fetal calf serum [13]. *T. brucei* PCF were grown at 28 °C in medium SDM-79 [14] supplemented with haemin (7.5 mg/l) and 10% heat-inactivated fetal-calf serum.

2.3. Genomic DNA purification and molecular cloning

In order to clone the MCP gene from *T. brucei* Lister 427, two synthetic oligonucleotide primers were designed: ATG (5′-GGATCCatgaagggcatacaaagagctcg-3′) and STOP (5′-GAATTCtcagttggcatcgtcacggtag-3′). PCR amplification was carried out using genomic DNA as template. PCR conditions were as follows: initial denaturation (5 min at 94 °C), denaturation (1 min at 94 °C), annealing (45 s at 62 °C) and elongation (90 s at 72 °C) followed by a final extension step (10 min at 72 °C). The PCR products were purified from a 1% agarose gel, using the QiaQuick protocol (Qiagen) and cloned into pGEM-T Easy vector (Promega). Sequencing of the products was performed using an ABI 377 DNA sequencer (PerkinElmer).

Site-directed mutations were introduced into the *Tb*MCP-1 gene cloned in the plasmid pGEX 2T, using the QuickChange™ site-directed mutagenesis kit (Stratagene).

DNA was obtained from PCF of *T. brucei* by using the Proteinase K/phenol/chloroform method [15].

2.4. Expression and purification of TbMCP-1 fused to glutathione S-transferase (GST)

The *T. brucei* MCP-1 gene (*Tb*MCP-1) was excised as BamHI/EcoRI fragment from pGEM-T Easy plasmid (Promega), gel purified and subcloned into the BamHI and EcoRI sites of the pGEX 2T expression vector. The resulting construct presented a GST tag at the N-terminus with a thrombin cleavage site. The construct was transformed into *E. coli* BL21 Codon Plus (DE3) cells. GST fusion protein was expressed by induction of exponential phase cultures (A_{600} = 0.6) with 0.5 mM IPTG for 12 h at 18 °C with vigorous (250 rpm) shaking. Bacteria were harvested by centrifugation at 5000 × *g* for 30 min at 4 °C, resuspended in 50 mM Tris–HCl pH 7.6, 150 mM NaCl, 0.1% Triton X-100, 1 mM PMSF and 1 mg/ml lysozyme, and centrifuged at 12,000 × *g* for 30 min at 4 °C to obtain the bacterial crude extract.

The recombinant *Tb*MCP-1 fusion protein was purified using a glutathione-agarose resin (GE) equilibrated with 50 mM Tris–HCl pH 7.6 containing 150 mM NaCl. The column was washed with 10 column vol. of the equilibration buffer and the sample was eluted with 50 mM Tris–HCl pH 7.6, 150 mM NaCl containing 10 mM reduced glutathione. Samples were desalted using a PD-10 column (GE) according to the manufacturer's specifications. Protein purity was evaluated on a Coomassie Blue-stained SDS 10% polyacrylamide gel. A 6xHis-tagged version of *Tb*MCP-1 was constructed as in the case of *Tc*MCP-1 [6], and the recombinant enzyme was purified by IMAC-Ni^{2+}. This recombinant *Tb*MCP-1 was very unstable, but could be used to exclude the influence of the GST tag in enzyme dimerization and kinetics. Recombinant *Tc*MCP-1 from *T. cruzi* was purified as described in [5].

2.5. Enzyme assays

Routinely, recombinant *Tb*MCP-1 activity was assayed using furyl-acryloyl (FA)-Ala-Lys (200 μM) as substrate in 100 mM MOPS pH 7.3. Initial steady-state velocity was determined by continuous assay for a range of substrate concentrations at 340 nm with a Beckman DU 650 spectrophotometer. One unit of activity was defined as the amount of enzyme that released 1 μmol of the residue being cleaved per min at 25 °C. Kinetic parameters for recombinant *Tb*MCP-1 were also determined using FA-Ala-Lys in 100 mM MOPS buffer, pH 7.3.

The substrate preference with respect to P1′ position was determined using benzyloxycarbonyl-Ala-X (ZAX) substrates (Bachem and Sigma), using the ninhydrin method for detection [16]. The reaction mixture contained 6 mM ZAX substrate in 100 mM MOPS,

pH 7.3. One enzyme unit was defined as the amount of enzyme that produced a ninhydrin-positive substance corresponding to 1 μmol of amino acid per min.

The substrate specificity with respect to P2 and P1 positions was determined using a series of fluorescence-quenched tripeptides [17]. Enzymatic activity was continuously followed with an AMINCO®–Bowman Series 2 Spectrofluorimeter by measuring the fluorescence at 320 nm (λ_{ex}) and 420 nm (λ_{em}). The slope was converted into micromoles of substrate hydrolyzed per minute based on a calibration curve obtained from complete hydrolysis of each peptide.

2.6. Effects of pH, metal ions and general inhibitors

For the determination of the optimum pH, the enzyme activity was determined in the following buffers at 100 mM: MES (pH 5–6.7), MOPS (pH 6.5–7.9) and HEPES (pH 7–8.2). Metal-ion-dependence and inhibition pattern were investigated by assaying the purified recombinant peptidase activity after pre-incubation with different metal chlorides ranging from 1 μM to 1 mM or the chosen inhibitor. In all cases the reaction mixture contained 200 μM FA-Ala-Lys in 100 mM MOPS, pH 7.3.

2.7. Gel-filtration experiments

These experiments were conducted using a Superose 12HR 10/30 (Pharmacia Biotech) column in an Äkta Purifier System (GE). The sample was eluted with 50 mM Tris–HCl containing 200 mM NaCl. The enzyme activity was assayed with 200 μM FA-Ala-Lys in 100 mM MOPS pH 7.3. The molecular-mass markers used were vitamin B12 (1.3 kDa), myoglobin (17 kDa), ovalbumin (44 kDa), BSA (66 kDa), and γ-globulin (158 kDa).

2.8. Antibody generation

Anti-*Tb*MCP-1 polyclonal antibodies were obtained by immunizing mice with three doses (15 days apart) of the purified *Tb*MCP-1 recombinant protein (subcutaneous injection). Each mouse received a first dose consisting of 20 μg of antigen with Freund's complete adjuvant (1:1) and other three doses, 5 μg each, with Freund's incomplete adjuvant. After the mice were bled, the serum was separated by centrifugation at 3000 × *g* and kept frozen at −20 °C until use.

2.9. Western blot analysis

The expression pattern in the different stages of the life cycle of *T. brucei* was analyzed by Western blot. Parasites (20×10^6 cells) were resuspended in cracking buffer, submitted to 10% SDS-PAGE and then transferred onto a nitrocellulose Hybond ECL membrane (GE). The membrane was blocked with 3% (w/v) non-fat milk and 2% glycine in TBS (50 mM Tris–HCl pH 7.6 containing 150 mM NaCl) for 30 min and incubated with anti *Tb*MCP-1 serum (1:100, 1 h) diluted in blocking solution. It was then washed with TBS for 20 min, with 0.05% NP40 in TBS for 10 min, and with TBS for 10 min. After that, it was incubated with horseradish-peroxidase-conjugated goat anti mouse IgG (Sigma) (1:5000, 1 h) in blocking solution. Blots were washed as before and developed with Super-Signal WestPico Chemiluminescent Substrate (Pierce).

2.10. Immunofluorescence experiments

To determine the subcellular localization of *Tb*MCP-1 in BSF, 1×10^6 parasites were washed with TD Buffer (0.025 M KCl, 0.4 M NaCl, 0.005 M $MgSO_4$, 0.1 M Na_2HPO_4, 0.01 M NaH_2PO_4, 0.1 M glucose), fixed with paraformaldehyde (PFA) 4% in PBS pH 7.6 for 1 h at room temperature and then attached to poly-lysine coated glass coverslips (30 min). Parasites were permeabilized with 0.3% Triton-X-100 in PBS, pH 7.4 for 30 s, washed 3 times with PBS pH 7.4 and incubated with blocking solution (50 mM NH_4Cl, 3% BSA, 5% goat serum, 1% fish gelatin in PBS pH 7.4) for 1 h at room temperature. Incubation with primary antibody (1:150 in 1% BSA pH 8) was made for 1 h. Coverslips were washed three times with PBS for 1 min. Alexa Fluor® 488-conjugated goat anti-mouse (Molecular Probes) (1:1000 for 1 h) was used as secondary antibody. Coverslips were washed again three times with PBS and then mounted using 15 μl of Fluor Save (Calbiochem). Nucleus and kinetoplast were stained with DAPI (4′,6-diamidino-2-phenylindole) (5 mg/ml).

PCF were air-dried on poly(L-lysine)-coated glass coverslips, fixed with 4% (w/v) PFA in PBS (20 min), incubated with 25 mM NH_4Cl (10 min) and permeabilized with 2% BSA, 0.1% saponin, 2% normal goat serum in PBS (30 min). The antibodies were diluted in blocking solution and incubation conditions were the same as with the BSF. Samples were examined with a Nikon Eclipse E600 microscope and photographed with a digital Sport RT Slider camera.

2.11. Activity of TbMCP-1 on vasoactive peptides

Bradykinin (BK, RPPGFSPFR, 1061 Da) and angiotensin I (Ang I, DRVYIHPFHL, 1296 Da) were used at 10 pmol/μl in buffer 10 mM MOPS pH 7.3 (*Tb*MCP-1) or 10 mM MES, pH 6.2 (*Tc*MCP-1). At different times, the reaction was stopped by mixing one volume of the sample with one volume of 0.1% α-ciano-4-hidroxycinnamic acid (in 50% acetonitrile). Samples were seeded in a Ground Steal plate (Bruker Daltonics) and analyzed by MALDI-TOF mass spectrometry (Ultraflex, Bruker Daltonics).

3. Results

3.1. The genome of T. brucei encodes a single M32 MCP

Within the trypanosomatidae family, the peptidase family M32 seems to have followed different evolutive pathways. Thus, *T. cruzi* genome encodes two different M32 MCPs (*Tc*MCP-1 and *Tc*MCP-2), which are regulated throughout the parasite life cycle [6]. *Leishmania* spp., on the other hand, present multiple M32 paralogs and pseudogenes [6], all of them homologs of *Tc*MCP-1. Most of them are species specific. In contrast, the related parasite *T. brucei* appears to have reduced to a minimum the M32 protein repertoire. Analysis of the genomic data of this organism led us to identify a single M32 homolog. This enzyme, named *Tb*MCP-1, shares 72% identity to the characterized *Tc*MCP-1 and displays the highest sequence identity (47–33%) with those M32 proteins of the proteobacteria group. Fig. 1 shows the schematic representation of the conserved M32 peptidase motifs found in *Tb*MCP-1 including the canonical HEXXH sequence that contains the active-site glutamic acid residue at position 268 [4], flanked by two histidine residues (positions 267 and 271) that coordinate the catalytic metal ion.

3.2. Expression, purification and biochemical characterization of recombinant TbMCP-1

The M32 MCPs characterized to date differ in various aspects, including gene copy number, substrate specificity and pattern of expression. To address these aspects on the only M32 family member present in *T. brucei*, we analyzed its enzymatic properties. Thus, the full-length *Tb*MCP-1 gene was cloned into the bacterial expression vector pGEX 2T, and expressed in *E. coli* BL21 Codon Plus (DE3) cells as an N-terminally GST-tagged recombinant enzyme. *Tb*MCP-1 was purified in one step using a glutathione–agarose resin with a yield of 9.6 mg/l of bacterial culture. Recombinant *Tb*MCP-1

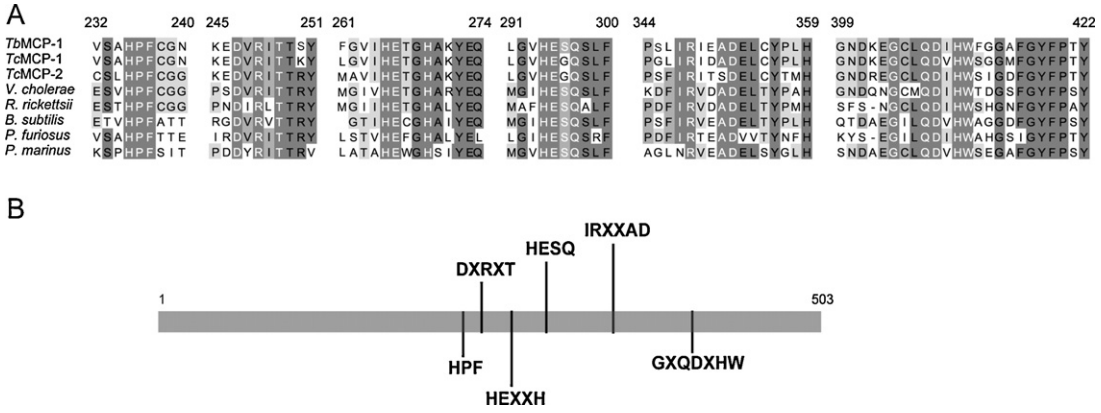

Fig. 1. (A) In the alignment, sequences were sorted by similarity to *Tb*MCP-1 using the CLUSTALW program. Similar residues according to the BLOSUM62 matrix are indicated by different tones of gray, according to the degree of similarity. Accession numbers with percent of identity to *Tb*MCP-1 are as follows: *Tc*MCP-1, CAG28317.1, 71%; *Tc*MCP-2, CAG28318.1, 59%; *Vibrio cholerae* O1 biovar eltor str. N16961, NP_231057, 47%; *Rickettsia rickettsii*, ZP_00153287, 33%; *Bacillus subtilis* subsp. subtilis str. 168, NP_390090, 33%; *Pyrococcus furiosus*, 1KA4_A, 28% and *Prochlorococcus marinus* subsp. pastoris str. CCMP1986, NP_892611, 28%. (B) Schematic representation of the conserved M32 family motifs.

was evaluated for purity on Coomassie Blue stained 7.5% polyacrylamide gel. The apparent subunit molecular mass of the purified enzyme was in good agreement with the calculated mass of the affinity-tagged product of the corresponding gen (approx. 77 kDa, Fig. 2A). As *T. cruzi* MCPs, *Tb*MCP-1 eluted in a single peak from a Superose 12HR 10/30 column with an apparent molecular mass corresponding to 159 kDa, indicating that the enzyme associates into catalytically active homodimers (Fig. 2B). A possible role of the GST tag in dimerization was excluded by repeating the experiment with a 6xHis-tagged recombinant enzyme, which gave an approximate value of 106 kDa.

In order to analyze the expression pattern of *Tb*MCP-1 along the parasite life cycle, we obtained polyclonal antibodies against the recombinant enzyme. Western blot analysis employing whole parasite extracts demonstrated that *Tb*MCP-1 is expressed in both mammal and insect stages (Fig. 3A). This pattern of expression is similar to that of *Tc*MCP-1, and contrasts with those of other MCPs found in *T. cruzi* and *Leishmania major* which were restricted to the insect stages [6,18]. The subcellular localization of the *T. brucei* enzyme was studied by indirect immunofluorescence. Using the polyclonal antiserum raised against recombinant *Tb*MCP-1 we obtained a diffuse uniform fluorescence throughout the cytosol of both procyclic and bloodstream forms of the parasite (Fig. 3B and C).

The purified recombinant *Tb*MCP-1 was used in enzymatic assays with N-blocked furylacryloyl dipeptides commonly employed for screening carboxypeptidases. These experiments revealed that the *T. brucei* enzyme exhibits a significant hydrolytic activity against the carboxypeptidase B (CPB, subfamily M14B) substrate FA-Ala-Lys at an optimal pH 7.0–7.8 (Supplementary Figure 1). The FA-Phe-Phe dipeptide, on the other hand, was not cleaved (Table 1).

Metal-ion chelators EDTA (10 mM) and *o*-phenanthroline (10 mM) were strong inhibitors, consistent with the *Tb*MCP-1 being a metal-dependent enzyme (Table 2). Carboxypeptidase B-like inhibitors such as the arginine analog GEMSA or Plummer's inhibitor were also effective whereas DL-benzylsuccinic acid, a potent inhibitor of carboxypeptidase A, was less effective. Although M32 MCPs have a similar fold to that of the angiotensin I-converting enzyme (ACE1), a dipeptidyl peptidase of the family M2, the specific ACE1 inhibitor captopril had no effect on *Tb*MCP-1 (Table 2). On the other hand, DX600, a commonly used ACE2 inhibitor [19], presented a modest inhibition on *T. brucei* enzyme most likely due to a non optimal amino acid sequence. It is noteworthy that

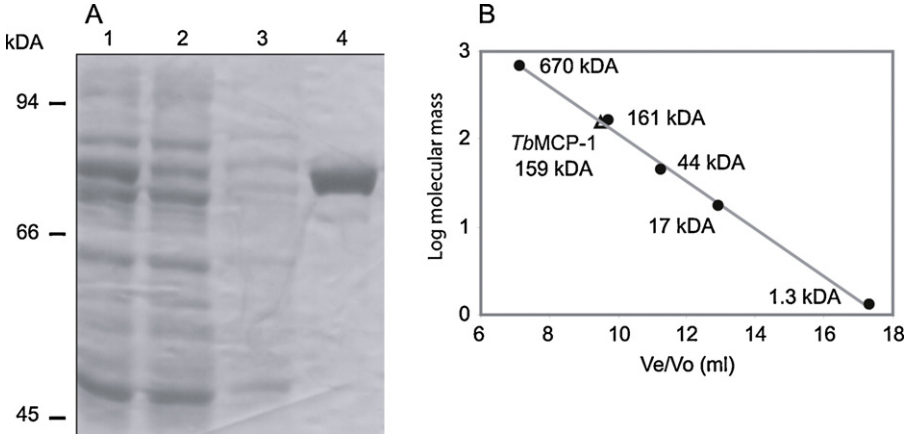

Fig. 2. (A) 7.5% SDS-PAGE showing the different fractions of the *Tb*MCP-1 purification stained with Coomassie blue. Lane 1, crude extract obtained from the disruption of induced *E. coli* cells; lane 2, glutathione-agarose eluate; lane 3, GST-agarose washes with 50 mM Tris–HCl pH 7.6, 150 mM NaCl; lane 4, purified *Tb*MCP-1 eluted with 50 mM Tris–HCl pH 7.6, 150 mM NaCl, 10 mM reduced glutathione. (B) The molecular mass of active *Tb*MCP-1 was determined by molecular exclusion chromatography on a Superose 12HR 10/30 column: *Tb*MCP-1 (▲), molecular mass markers (●) [thyroglobulin (670 kDa), γ-globulin (158 kDa), ovalbumin (44 kDa), myoglobin (17 kDa) and vitamin B12 (1.3 kDa)].

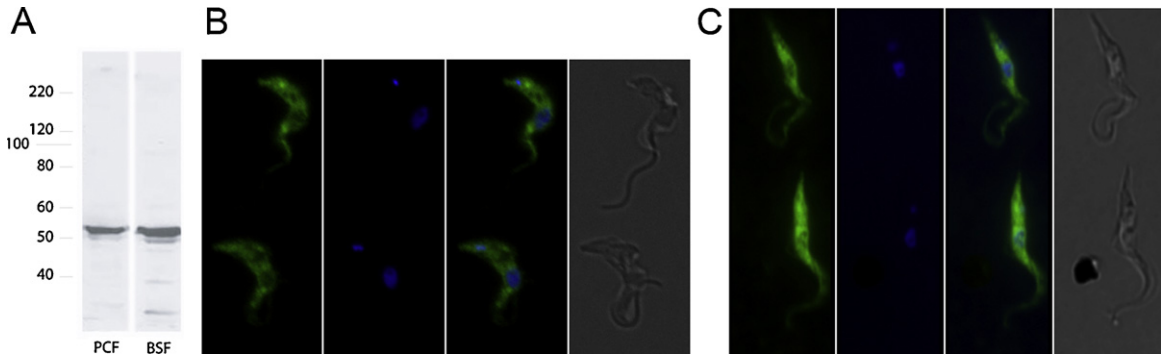

Fig. 3. (A) Western blot showing expression of *Tb*MCP-1 in vector (PCF) and host (BSF) stages of the parasite. The apparent molecular mass of the native enzyme (approx. 55 kDa) was in good agreement with the mass calculated from the corresponding gene (approx. 57.7 kDa). (B) Immunofluorescence showing subcellular localization of the enzyme in the bloodstream form (green). (C) Immunofluorecence showing subcellular localization of the enzyme in the procyclic stage of the parasite. Nucleus and kinetoplast were stained with DAPI (blue). Figures were prepared using the program ImageJ 1.46b.

*Tc*MCP-1 was similarly insensitive to captopril and partially inhibited (residual activity 22.5%) by the same concentration of DX600 (not shown).

As for *Tc*MCP-1, the presence of Co^{2+} inhibited *Tb*MCP-1 activity on FA-Ala-Lys substrate. The residual activity measured in the presence of 10 μM $CoCl_2$ was 16 ± 7%. Mn^{2+} had also effect but at a higher concentration, the residual activity being 18 ± 5% with 100 μM $MnCl_2$. Ca^{2+} and Mg^{2+} ions also resulted inhibitory (72 ± 3 and 65 ± 3 were the residual activities, respectively, when measured in the presence of 100 μM of the corresponding metal chloride). Ni^{2+} and Zn^{2+}, two strong inhibitors of *Tc*MCP-1, had no effect on the *T. brucei* enzyme.

3.3. P1′ preference

To further characterize the substrate preference with respect to the P1′ position of the identified *Tb*MCP-1, several commercially available ZAX (where X position was successively occupied with 1 of 17 amino acids) substrates were used. As shown in Supplementary Figure 2, the recombinant *Tb*MCP-1 acted best on substrates having a basic residue at P1′ position. Maximum activity was found with ZAK (0.28 μmol/min mg). ZAR and ZAM were also hydrolyzed, although the relative activity on these peptides was lower (37.1% and 18.3%, respectively, when compared with the ZAK substrate). Other polar C-terminal residues including His, Tyr, Ser and Asn, and the aliphatic Leu, where cleaved at a lower extent.

3.4. Kinetic parameters

The kinetic parameters of *Tb*MCP-1 were evaluated using the FA-Ala-Lys substrate in 100 mM MOPS, pH 7.3. A possible effect of the GST tag on the kinetic parameters was excluded by determining the K_m for this substrate with a 6xHis-tagged recombinant enzyme, which was 239 μM. As shown in Table 1, *Tb*MCP-1 has less affinity for this dipeptide than *Tc*MCP-1, although its catalytic efficiency is higher. Replacement of Glu268 (active-site glutamic acid residue) or Arg348 (residue involved in COOH terminal binding) by an alanine residue resulted in complete loss of activity.

Table 1
Kinetic parameters of *Tb*MCP-1.

Enzyme	FAAlaLys			FAPhePhe		
	K_m (mM)	k_{cat} (s^{-1})	k_{cat}/K_m (s^{-1}/mM)	K_m (mM)	k_{cat} (s^{-1})	k_{cat}/K_m (s^{-1}/mM)
*Tb*MCP-1	0.260	32	123	N.D.	–	–
*Tb*MCP-1 M304R	0.240	8.6	36	0.033	2.5	76
*Tb*MCP-1 E268A	N.D.	–	–	–	–	–
*Tb*MCP-1 R348A	N.D.	–	–	–	–	–
*Tc*MCP-1[a]	0.144	10	69	N.D.	–	–
*Tc*MCP-1 M304R[a]	N.D.	–	–	0.011	0.3	27
*Tc*MCP-2[a]	N.D.	–	–	0.019	1.2	63

N.D.: not detected under these measurement conditions.
[a] Data from Ref. [6].

Table 2
Effect of different inhibitors on *Tb*MCP-1 activity.

Inhibitor	Concentration	Type	Residual activity (%)
–			100 ± 9.9
EDTA	10 mM	Metallo-proteases, metal activated proteases	8.7 ± 1.2
o-Phenanthroline	10 mM	Metallo-proteases, metal activated proteases	0
PMSF	1 μM	Serine proteases	93 ± 24
E64	5 μM	Cysteine proteases	85 ± 3.7
Pestatin A	1 μM	Some aspartic proteases	89 ± 4.1
Captopril	5 μM	M2 dipeptidilpeptidases (ACE1)	114 ± 39
DX600	12.5 μM	M2 carboxypeptidase (ACE2)	60.3 ± 6.7
GEMSA	5 μM	Carboxypeptidases B-*like*	9.1 ± 1.2
Plummer's inhibitor	5 μM	Carboxypeptidases B-*like*	6.8 ± 3.8
DL-benzylsuccinic acid	5 μM	Carboxypeptidases A-*like*	33 ± 16

Previous studies suggested that Met at position 304 could favor B-type substrate utilization [5]. In order to test this hypothesis Met304 present in *Tb*MCP-1 was replaced by an Arg (residue found in the carboxypeptidase A-like *Tc*MCP-2). Table 1 shows that the inclusion of an Arg in that position confers *Tb*MCP-1 activity towards the FA-Phe-Phe substrate, thus confirming a role of this residue in substrate specificity.

3.5. FRET substrates

Fluorescence Energy Resonance Transfer (FRET) peptides are an excellent alternative for enzyme kinetic studies and for analysis of the enzymatic activities in biological fluids, crude tissue extracts or on the surface of cells in culture [20]. As a consequence we decided to evaluate the activity of *Tb*MCP-1 on a FRET peptide series containing a free C-terminal group [21]. Table 3 summarizes the activity of the recombinant *T. brucei* enzyme on these fluorogenic tripeptides. The fixed modified Lys residue at P1′ position led us to evaluate the effect of the amino acid present at P1 and P2 positions which strongly influence the efficiency of the enzyme. For comparative reasons, *Tc*MCP-1 was also included in the experiment. This enzyme showed a slightly different substrate preference as compared with *Tb*MCP-1, although the hydrolytic activity of the enzyme was also affected by the amino acid residues present in P1 and P2 positions. Notably neither the *T. brucei* nor the *T. cruzi* enzyme could hydrolyze Abz-ARK(Dnp)-OH, probably due to the presence of an Ala residue at P2 position. The inclusion of a Val residue in P1 only abolished the activity of *Tb*MCP-1, whereas *Tc*MCP-1 showed activity against this substrate (Table 3).

3.6. Mapping TbMCP-1 substrate specificity determinants by site-directed mutagenesis

In order to explain the lack of activity of *Tb*MCP-1 on Abz-FVK(Dnp)-OH we submitted the amino acid sequence of this enzyme to the SWISS-MODEL comparative protein modeling server [22]. Using *Tc*MCP-1 crystal structure as template we determined which residues in the *Tb*MCP-1 substrate binding channel differ from the corresponding residues in the *T. cruzi* enzyme. Only five changes were found: K91L, R288M, F411S, I408V and A414M (Fig. 4). To investigate the hypothesis that residues at these positions might be responsible for the lack of activity, site-directed mutations were introduced into this enzyme. Of the five point mutants constructed, only the replacement of Ala414 with Met resulted in the appearance of activity of *Tb*MCP-1 on Abz-FVK(Dnp)-OH. The affinity of the mutant enzyme (K_m 0.21 μM) on Abz-FVK(Dnp)-OH was similar to the one of the wild-type *Tc*MCP-1, although the k_{cat} was lower (0.01 s^{-1}). These results suggest that this residue is part of the S1 subsite.

3.7. Protozoan MCPs are active on bioactive peptides

Contrary to other previously characterized M32 peptidases, the protozoan enzymes seem to have a marked substrate preference at P1′ position. Moreover, the nature of the amino acid residue present at P1 or P2 also affects the hydrolytic efficiency of both enzymes as shown in Section 3.5. To explore these effects on natural peptides we employed two vasoactive compounds, BK (RPPGFSPFR) and Ang I (DRVYIHPFHL). As shown in Supplementary Figures 3 and 4, after 30 min of digestion *Tc*MCP-1 solely produces Des-Arg9-BK (RPPGFSPF↓R), a B-type agonist of B1 receptors, whereas the *T. brucei* enzyme generates a mixture of BK (1–7) (RPPGFSP↓F↓R) and Des-Arg9-BK, which is eventually fully converted to BK (1–7).

The final products of Ang I hydrolysis are also different for both MCPs, thus *Tb*MCP-1 mainly produced Ang II (DRVYIHPF↓H↓L) through the sequential removal of the last two amino acid residues of the peptide, whereas the *T. cruzi* enzyme produces a mixture of Ang (1–9), Ang II and Ang (1–7). According to these results *Tb*MCP-1 generates the same products that ACE would produce acting on these peptides.

4. Discussion

We report herein the identification and biochemical characterization of the only M32 MCP present in the *T. brucei* genome. This enzyme is expressed in the cytosol of both mammal and insect stages of the parasite. Interestingly, this is the only M32 peptidase that has orthologs in the TriTryps genomes. *Tc*MCP-1, the *Tb*MCP-1 counterpart described in *T. cruzi*, also presents a similar pattern of expression and *in vitro* utilizes the CPB substrate FA-Ala-Lys [6]. These features contrast with those of species-specific M32 MCPs found in *L. major* and *Tc*MCP-2, an enzyme of *T. cruzi* with CPA-like substrate preference, these enzymes being restricted to the insect stages [6,18].

Previous studies have shown that M32 MCPs could hydrolyze a broad spectrum of amino acid residues at P1′ [3,16,18,23]. On the other hand, the recombinant *T. brucei* enzyme described here presented a marked substrate preference for basic residues (Lys and Arg). This characteristic is more reminiscent to *Bacillus subtilis* CP, an M32 MCP reported to act over a few substrates including ZAK and ZAR [24]. The use of internally quenched fluorogenic tripeptides has also pointed out the effect of the amino acid residue located at P1 and P2 positions (and so the selectivity of the S1 and S2 subsites). These aspects were not previously analyzed for this group of enzymes. Our results suggest that trypanosomatid MCPs act with a different efficiency on the substrates of this series, these differences being more marked for *Tb*MCP-1. An explanation of this could be found in the structure. Several crystallographic structures of M32 family members have been published [4,5,24]. However, none of them was determined in the presence of a substrate or inhibitor, and thus the putative substrate binding sites are still unknown.

Table 3
Kinetic parameters of *Tb*MCP-1 and *Tc*MCP-1 on fluorescence-quenched tripeptide substrates.

Substrate	*Tb*MCP-1			*Tc*MCP-1		
	K_m (μM)	k_{cat} (s^{-1})	k_{cat}/K_m (s^{-1}/μM)	K_m (μM)	k_{cat} (s^{-1})	k_{cat}/K_m (s^{-1}/μM)
Abz-ARK(Dnp)-OH	N.D.	–	–	N.D.	–	–
Abz-HRK(Dnp)-OH	1.8	0.503	0.279	>10	–	–
Abz-LRK(Dnp)-OH	2.7	0.012	0.004	4.4	0.156	0.036
Abz-ERK(Dnp)-OH	2.2	0.010	0.005	>10	–	–
Abz-FRK(Dnp)-OH	1.1	1.374	1.249	2.9	0.346	0.119
Abz-FSK(Dnp)-OH	0.3	0.013	0.043	5.4	0.032	0.006
Abz-FHK(Dnp)-OH	3.0	2.159	0.720	5.4	0.886	0.164
Abz-FVK(Dnp)-OH	N.D.	–	–	0.3	0.153	0.510
Abz-FPK(Dnp)-OH	0.3	0.004	0.013	1.9	0.004	0.002

N.D.: not detected under these measurement conditions.

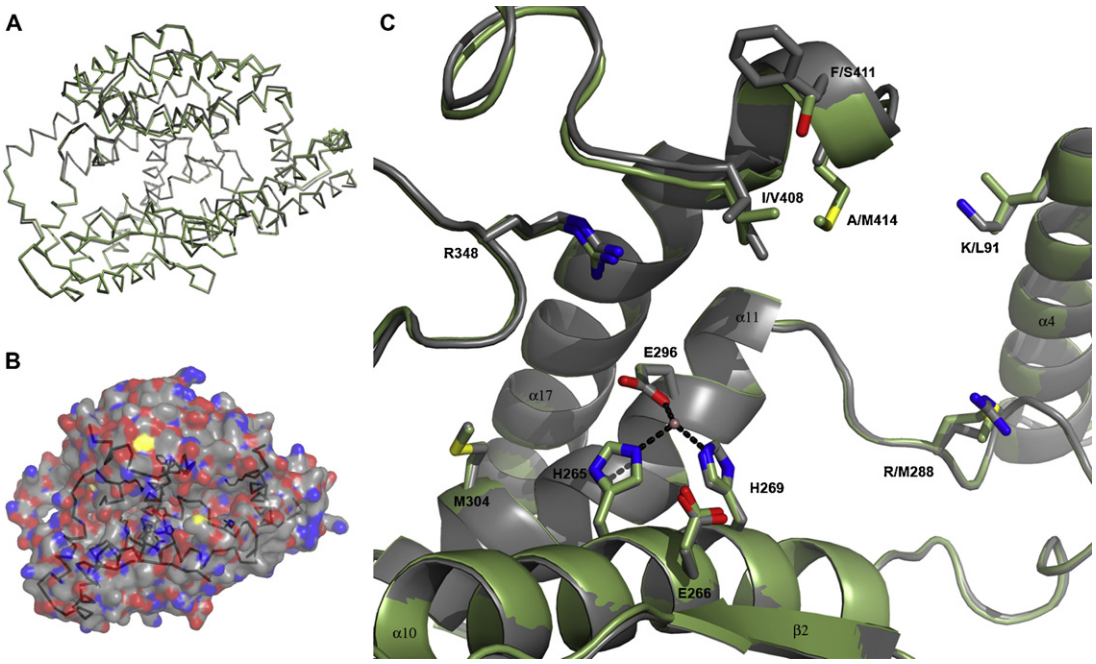

Fig. 4. Homology models of *Tb*MCP-1 based on the crystal structure of *Tc*MCP-1 (pdb id 3dwc) were utilized to map the positions of the potentially critical residues involved in substrate specificity. (A) Superimposed C-α ribbon of a single *Tc*MCP-1 subunit (green) and *Tb*MCP-1 (gray). (B) Surface diagram of *Tb*MCP-1 subunit. (C) Close-up view of protozoan MCP active-site cleft. Residues relevant for catalysis as well as residues that differ between both enzymes are shown as sticks. Colour-code; blue for nitrogens, yellow for sulfurs, and red for oxygens. The catalytic metal ion of the protozoan enzymes is depicted as a pink. Figures were prepared using the program PyMOL. (The PyMOL Molecular Graphics System, Version 1.3, Schrödinger, LLC.)

Moreover, the role that some residues play in catalysis has been suggested but has not been confirmed. In this direction, we had pointed out the relevance of Arg348. This residue, proposed to form a salt bridge with the C-terminal carboxylate group of the bound substrate [4,5] is essential since its replacement by an Ala abolished the enzyme activity. Arg348 is structurally conserved in other monocarboxypeptidases of the clan MA, namely, ACE2. In particular, the crystal structure of ACE2, revealed that the guanidino group of Arg273 (the equivalent residue of Arg348) made a bidentate H-bond with the terminal carboxylate of the inhibitor MLN-4760 [25]. Further, its larger size, compared with Gln present in ACE, was suggested to eliminate the S2′ subsite in ACE2 [26]. Two major implications were derived from this single residue change. First, the switch in the peptidyl dipeptidase activity of ACE to the observed carboxypeptidase activity of ACE2 and second, why the potent ACE inhibitors such as lisinopril, enalaprilat, and captopril are inactive against ACE2 [25]. Thus, for both *Tb*MCP-1 and *Tc*MCP-1, not only this essential Arg residue is conserved compared with ACE2, but also the response to some inhibitors. Two other residues, Met304 and Ala414, were found to influence the substrate specificity. In the case of Met304, previous work has suggested that this residue could favor B-type substrate utilization [5]. In the case of the *T. brucei* enzyme, its replacement by a positively charged residue resulted in the appearance of activity towards the FA-Phe-Phe substrate, with the concomitant reduction of the catalytic efficiency over FA-Ala-Lys. Although the effect of this substitution is not as dramatic as it has been reported for *Tc*MCP-1 [5], which completely lost the activity on basic substrates when the same mutation was introduced, it is clear that this residue plays a major role in A/B-type substrate discrimination. Due to its orientation respect to the catalytic Glu, this residue may be part of the S1′ subsite. The second residue studied was Ala414. This residue located in the vicinity of the proposed S1 pocket is entirely responsible for the lack of activity of *Tb*MCP-1 over the Abz-FVK(Dnp)-OH substrate since the introduction of a Met confers the *T. brucei* enzyme the ability to act on this peptide. Thus, in spite of having 72% identity, in MCP-1 like enzymes a few single amino acid residues changes can cause significant changes in substrate utilization.

No biological function has yet been assigned to M32 peptidases. On the bases of their biochemical properties and stage-specific expression, it has been suggested that protozoan MCPs might play a role in peptide catabolism [18]. In particular, Isaza and co-workers suggested that a species-specific M32 MCP found in *L. major* could facilitate the growth of the promastigote form of the parasite participating in the degradation of peptides and proteins to free amino acids [18]. Other possible functions came from the structural similarity of this family with mammalian metallopeptidases, including ACE and ACE2 [5]. Both enzymes are zinc peptidases that play a central role in the renin–angiotensin system. Taking into account the marked substrate preference reported for some M32 MCPs a regulatory role in the metabolism of small peptides could not be excluded. In this direction, we have shown that *Tc*MCP-1 could produce exclusively des-Arg bradykinin by hydrolysis of bradykinin *in vitro*. This peptide was reported to facilitate *T. cruzi* cell invasion through B1 receptors since addition of [Leu8]-des-Arg9-BK, a B1 receptor antagonist, is known to reduce the parasite infectivity [27]. In the case of *T. brucei*, the kallikrein-kinin system was reported to be severely dysregulated in trypanosome-infected hosts [28]. Thus, *Tb*MCP-1 could be a good candidate to influence the activity of host vasoactive kinins. Moreover, there is recent evidence that suggests that M32 peptidases are secreted by trypanosomatids [29,30] making the latter hypothesis feasible. In fact, it has been reported that a pyroglutamyl peptidase released by *T. brucei* could modulate plasma neuropeptide levels of infected hosts *in vitro* and *in vivo* [31]. Alternatively *Tb*MCP-1 might be released *in vivo* by dead or dying trypanosomes lysed in the circulation by the various antimicrobial host defense mechanisms. This is probably the case of *T. brucei* oligopeptidase B, an enzyme whose activity is found in the plasma of infected rats and, as *Tb*MCP-1, does not contain any known secretion sequences. The authors hypothesize that the last explanation

is the most plausible one [32]. Thus, trypanosome-derived peptidases, including *Tb*MCP-1, could play a role in modulating peptide hormone dynamics in the plasma of infected hosts, having significant implications for our understanding of the lesions observed in African trypanosomiasis.

5. Conclusions

T. brucei contains only one member of the M32 metallopeptidase family, *Tb*MCP-1. This enzyme has similar properties when compared with its orthologue in *T. cruzi*, *Tc*MCP-1, but also has significant differences in its response to divalent cations and in substrate specificity. The ability of *Tb*MCP-1 to act on bradykinin and angiotensin I open up the possibility of a role of the enzyme in the pathogenesis of Sleeping Sickness, which might make it a suitable target for the development of new chemotherapeutic agents.

Acknowledgements

JJC is a member of the research career of the Argentinian National Research Council (CONICET); GTN has a post-doctoral fellowship from CONICET; and APF has a fellowship from the grant "Parasitic Diseases Research at the IIB" (Grant # 1D43TW007888-01, Sub-award # RR374-041/350037, from FIRCA, NIH). The work performed in Argentina was financed by PICT 2006 02381 from the Agencia Nacional de Promoción Científica y Tecnológica (ANPCyT, MinCyT), Argentina. AKC and LJ were supported by the Brazilian agencies Fundação de Amparo a Pesquisa do Estado de São Paulo (FAPESP) and Conselho Nacional de Desenvolvimento Científico e Tecnológico (CNPq).

Appendix A. Supplementary data

Supplementary data associated with this article can be found, in the online version, at http://dx.doi.org/10.1016/j.molbiopara.2012.04.008.

References

[1] Vendrell J, Aviles FX. Carboxypeptidases. In: Turk V, editor. Proteases: new perspectives. Birkhäuser Verlag; 1999.
[2] Arolas JL, Vendrell J, Aviles FX, Fricker LD. Metallocarboxypeptidases: emerging drug targets in biomedicine. Current Pharmaceutical Design 2007;13:349–66.
[3] Lee SH, Minagawa E, Taguchi H, Matsuzawa H, Ohta T, Kaminogawa S, et al. Purification and characterization of a thermostable carboxypeptidase (carboxypeptidase Taq) from *Thermus aquaticus* YT-1. Bioscience, Biotechnology, and Biochemistry 1992;56:1839–44.
[4] Arndt JW, Hao B, Ramakrishnan V, Cheng T, Chan SI, Chan MK. Crystal structure of a novel carboxypeptidase from the hyperthermophilic archaeon *Pyrococcus furiosus*. Structure 2002;10:215–24.
[5] Niemirowicz G, Fernandez D, Sola M, Cazzulo JJ, Aviles FX, Gomis-Ruth FX. The molecular analysis of *Trypanosoma cruzi* metallocarboxypeptidase 1 provides insight into fold and substrate specificity. Molecular Microbiology 2008;70:853–66.
[6] Niemirowicz G, Parussini F, Aguero F, Cazzulo JJ. Two metallocarboxypeptidases from the protozoan *Trypanosoma cruzi* belong to the M32 family, found so far only in prokaryotes. Biochemical Journal 2007;401:399–410.
[7] Wilkinson SR, Kelly JM. Trypanocidal drugs: mechanisms, resistance and new targets. Expert Reviews in Molecular Medicine 2009;11:e31.
[8] Alvarez VE, Niemirowicz GT, Cazzulo JJ. The peptidases of *Trypanosoma cruzi*: digestive enzymes, virulence factors, and mediators of autophagy and programmed cell death. Biochimica et Biophysica Acta 2012;1824:195–206.
[9] Klemba M, Goldberg DE. Biological roles of proteases in parasitic protozoa. Annual Review of Biochemistry 2002;71:275–305.
[10] Dumas M, Bouteille B, Buguet A. Progress in Human African Trypanosomiasis. Sleeping Sickness. Springer; 1999.
[11] Puzer L, Cotrin SS, Cezari MH, Hirata IY, Juliano MA, Stefe I, et al. Recombinant human cathepsin X is a carboxymonopeptidase only: a comparison with cathepsins B and L. Biological Chemistry 2005;386:1191–5.
[12] Wirtz E, Leal S, Ochatt C, Cross GA. A tightly regulated inducible expression system for conditional gene knock-outs and dominant-negative genetics in *Trypanosoma brucei*. Molecular and Biochemical Parasitology 1999;99:89–101.
[13] Hirumi H, Hirumi K. Continuous cultivation of *Trypanosoma brucei* blood stream forms in a medium containing a low concentration of serum protein without feeder cell layers. Journal of Parasitology 1989;75:985–9.
[14] Brun R, Schonenberger. Cultivation and in vitro cloning or procyclic culture forms of *Trypanosoma brucei* in a semi-defined medium. Short communication. Acta Tropica 1979;36:289–92.
[15] Maniatis T, Fritsch EF, Sambrook J. Molecular cloning: a laboratory manual. 2nd ed. Cold Spring Harbor: Cold Spring Harbor Laboratory Press; 1989.
[16] Cheng TC, Ramakrishnan V, Chan SI. Purification and characterization of a cobalt-activated carboxypeptidase from the hyperthermophilic archaeon *Pyrococcus furiosus*. Protein Science 1999;8:2474–86.
[17] Bersanetti PA, Andrade MC, Casarini DE, Juliano MA, Nchinda AT, Sturrock ED, et al. Positional-scanning combinatorial libraries of fluorescence resonance energy transfer peptides for defining substrate specificity of the angiotensin I-converting enzyme and development of selective C-domain substrates. Biochemistry 2004;43:15729–36.
[18] Isaza CE, Zhong X, Rosas LE, White JD, Chen RP, Liang GF, et al. A proposed role for *Leishmania major* carboxypeptidase in peptide catabolism. Biochemical and Biophysical Research Communications 2008;373:25–9.
[19] Huang L, Sexton DJ, Skogerson K, Devlin M, Smith R, Sanyal I, et al. Novel peptide inhibitors of angiotensin-converting enzyme 2. Journal of Biological Chemistry 2003;278:15532–40.
[20] Carmona AK, Juliano MA, Juliano L. The use of Fluorescence Resonance Energy Transfer (FRET) peptides for measurement of clinically important proteolytic enzymes. Anais da Academia Brasileira de Ciencias 2009;81:381–92.
[21] Araujo MC, Melo RL, Cesari MH, Juliano MA, Juliano L, Carmona AK. Peptidase specificity characterization of C- and N-terminal catalytic sites of angiotensin I-converting enzyme. Biochemistry 2000;39:8519–25.
[22] Arnold K, Bordoli L, Kopp J, Schwede T. The SWISS-MODEL workspace: a web-based environment for protein structure homology modelling. Bioinformatics 2006;22:195–201.
[23] Lee HS, Kim YJ, Bae SS, Jeon JH, Lim JK, Kang SG, et al. Overexpression and characterization of a carboxypeptidase from the hyperthermophilic archaeon *Thermococcus* sp. NA1. Bioscience, Biotechnology, and Biochemistry 2006;70:1140–7.
[24] Lee MM, Isaza CE, White JD, Chen RP, Liang GF, He HT, et al. Insight into the substrate length restriction of M32 carboxypeptidases: characterization of two distinct subfamilies. Proteins 2009;77:647–57.
[25] Towler P, Staker B, Prasad SG, Menon S, Tang J, Parsons T, et al. ACE2 X-ray structures reveal a large hinge-bending motion important for inhibitor binding and catalysis. Journal of Biological Chemistry 2004;279:17996–8007.
[26] Guy JL, Jackson RM, Acharya KR, Sturrock ED, Hooper NM, Turner AJ. Angiotensin-converting enzyme-2 (ACE2): comparative modeling of the active site, specificity requirements, and chloride dependence. Biochemistry 2003;42:13185–92.
[27] Todorov AG, Andrade D, Pesquero JB, Araujo Rde C, Bader M, Stewart J, et al. *Trypanosoma cruzi* induces edematogenic responses in mice and invades cardiomyocytes and endothelial cells in vitro by activating distinct kinin receptor (B1/B2) subtypes. FASEB Journal 2003;17:73–5.
[28] Veenendaal GH, van Miert AS, van den IT, Scotman AJ, Zwart D. A comparison of the role of kinins and serotonin in endotoxin induced fever and *Trypanosoma vivax* infections in the goat. Research in Veterinary Science 1976;21:271–9.
[29] Geiger A, Hirtz C, Becue T, Bellard E, Centeno D, Gargani D, et al. Exocytosis and protein secretion in Trypanosoma. BMC Microbiology 2010;10:20.
[30] Silverman JM, Chan SK, Robinson DP, Dwyer DM, Nandan D, Foster LJ, et al. Proteomic analysis of the secretome of *Leishmania donovani*. Genome Biology 2008;9:R35.
[31] Morty RE, Bulau P, Pelle R, Wilk S, Abe K. Pyroglutamyl peptidase type I from *Trypanosoma brucei*: a new virulence factor from African trypanosomes that deblocks regulatory peptides in the plasma of infected hosts. Biochemical Journal 2006;394:635–45.
[32] Morty RE, Lonsdale-Eccles JD, Mentele R, Auerswald EA, Coetzer TH. Trypanosome-derived oligopeptidase B is released into the plasma of infected rodents, where it persists and retains full catalytic activity. Infection and Immunity 2001;69:2757–61.